

A MONTE CARLO STUDY OF THE "MINUS SIGN PROBLEM"  
IN THE t-J MODEL USING AN INTEL IPSC/860 HYPERCUBE

RECEIVED

SEP 23 1994

OSTI

M.D. KOVARIK AND T. BARNES

*Physics Division and Center for Computationally Intensive Physics,  
Oak Ridge National Laboratory, Oak Ridge, TN 37831-6373*

and

*Department of Physics, University of Tennessee,  
Knoxville, TN 37996-1200*

## ABSTRACT

We describe a Monte Carlo simulation of the 2-dimensional t-J model on an Intel iPSC/860 hypercube. The problem studied is the determination of the dispersion relation of a dynamical hole in the t-J model of the high temperature superconductors. Since this problem involves the motion of many fermions in more than one spatial dimensions, it is representative of the class of systems that suffer from the "minus sign problem" of dynamical fermions which has made Monte Carlo simulation very difficult. We demonstrate that for small values of the hole hopping parameter one can extract the entire hole dispersion relation using the GRW Monte Carlo algorithm, which is a simulation of the Euclidean time Schrödinger equation, and present results on  $4 \times 4$  and  $6 \times 6$  lattices. We demonstrate that a qualitative picture at higher hopping parameters may be found by extrapolating weak hopping results where the minus sign problem is less severe. Generalization to physical hopping parameter values will only require use of an improved trial wavefunction for importance sampling.

## 1. Introduction

Monte Carlo studies of dynamical fermion problems in more than one spatial dimension, such as the t-J model of the high temperature superconductors, are complicated by the "minus-sign problem" encountered in multifermion systems in more than one space dimension. For a general discussion of the minus sign problem see the paper of Loh *et al*<sup>1</sup>. This problem arises from the fact that off-diagonal matrix elements of the type

$$\langle n' | (I - H_I h_\tau) | n \rangle \quad (1)$$

MASTER

## **DISCLAIMER**

**Portions of this document may be illegible in electronic image products. Images are produced from the best available original document.**

can have either sign in these systems. These matrix elements are encountered for example in evolving an initial distribution of configurations to a ground-state distribution using the operator

$$e^{-H\tau} = \lim_{\substack{h_\tau \rightarrow 0 \\ n_\tau h_\tau = \tau}} \sum_{\{n\}} |n_\tau\rangle \langle n_\tau| (I - H h_\tau) |n_{\tau-1}\rangle \langle n_{\tau-1}| \dots \\ \dots |n_1\rangle \langle n_1| (I - H h_\tau) |n_0\rangle \langle n_0| \quad (2)$$

or in evaluating the partition function, which is the trace of this operator. The phases of these matrix elements may be assigned to weight factors associated with configurations generated by the algorithm, and these weights evidently can have either sign depending on the path  $\mathcal{S}(\tau)$  the configuration follows in Hilbert space. The weights are then used in averages in the calculation of matrix elements, which will have considerably larger statistical errors if weights occur with both signs in comparable numbers. In measuring dispersion relations using Monte Carlo techniques one encounters a related difficulty, which is that the matrix elements, Eq. (1), between momentum eigenstates are in general complex, so the "minus sign problem" generalizes to a "complex phase problem". Despite these difficulties recent Monte Carlo studies have found it possible to extract useful results for several systems which have minus-sign problems. These include the energy of the one-hole ground state in the t-J model<sup>2</sup> (which requires negative weights) and the dispersion relation of the spin-one Heisenberg chain<sup>3</sup> (which requires complex weights).

The t-J model<sup>4,5</sup>, which is the two-dimensional Heisenberg antiferromagnet on a square lattice with a hopping term, has attracted considerable interest as a candidate model of high temperature superconductivity. This model, defined by the Hamiltonian

$$H = -t \sum_{\langle ij \rangle, \sigma} (c_{i\sigma}^\dagger c_{j\sigma} + h.c.) + J \sum_{\langle ij \rangle} (\mathbf{S}_i \cdot \mathbf{S}_j - \frac{1}{4} n_i n_j), \quad (3)$$

incorporates the large antiferromagnetic interaction present in the copper-oxygen planes and allows hole hopping if vacancies are present.

In this paper<sup>6</sup> we show that the problem of determining t-J model dispersion relations using a Monte Carlo technique can be solved formally using complex weights. Although cancellations between weights do lead to a considerable increase in the statistical noise relative to Heisenberg model simulations in practice, one may nonetheless obtain interesting results for one-hole band structure using currently available computing facilities.

## 2. Method

We employ the "guided random walk" (GRW) algorithm, which was introduced by Barnes, Daniell and Storey<sup>7</sup> as a method in Hamiltonian lattice gauge theory, and has since been generalized to discrete degrees of freedom<sup>8,9</sup> and has been applied to U(1) lattice gauge theory<sup>10</sup>, to multi-quark systems in the nonrelativistic quark

model <sup>11</sup>, and to the Heisenberg antiferromagnet <sup>8,9,12-14</sup> and t-J<sub>z</sub> model <sup>15</sup>. In this method, the Euclidean time Schrödinger equation

$$-\frac{\partial}{\partial \tau} |\psi(\tau)\rangle = H |\psi(\tau)\rangle \quad (4)$$

generalizes to a diffusion equation with absorbers

$$-\frac{\partial}{\partial \tau} \rho(x, t) = -\kappa \nabla^2 \rho(x, t) + a(x) \rho(x, t) \quad (5)$$

when

$$H = -\frac{1}{2m} \frac{\partial^2}{\partial x^2} + V(x, t). \quad (6)$$

The diffusion equation is easily simulated using a random walk algorithm in which the probability of absorption is replaced by a weight factor.

The GRW algorithm is unlike GFMC in that it does not use a fluctuating population of "walkers", but instead generates a single unbranched random walk and associates a path-dependent weight factor with that walk. The weights of many such walks are then used in averages to determine energies, as we shall discuss. The weights can also be used in a straightforward manner to give *unbiased*  $|\psi_0|^2$ -weighted ground state matrix elements <sup>16</sup>, which is a difficult problem for some algorithms. (See Barnes, ref. 16, and Manousakis, ref. 17, for reviews of this and other algorithms used in studies of the Heisenberg model.)

In the GRW algorithm one generates a random walk in Hilbert space, in which the path followed by the configuration is parametrised by the Euclidean time  $\tau$ . One begins the random walk at  $\tau = 0$  with a chosen initial configuration (which in our case is a hole at (0,0) in a Néel state), and increments the Euclidean time in steps of  $h_\tau$ . After each time step the walk has the option of making a transition from the current configuration  $\mathcal{S}(\tau)$  to a new configuration  $\mathcal{S}'(\tau)$  with probability

$$P(\mathcal{S} \rightarrow \mathcal{S}') = r_{\mathcal{S}\mathcal{S}'} h_\tau, \quad (7)$$

where the stepping-rate matrix  $r_{\mathcal{S}\mathcal{S}'}$  is

$$r_{\mathcal{S}\mathcal{S}'} = \left| -\langle \mathcal{S}' | H_I | \mathcal{S} \rangle \frac{\Psi_0^g(\mathcal{S}')}{\Psi_0^g(\mathcal{S})} \right|; \quad (8)$$

after the  $\mathcal{S} \rightarrow \mathcal{S}'$  transition is attempted, the Euclidean time is incremented to  $\tau + h_\tau$ , and the process is repeated. In these formulas  $H_I$  is the off-diagonal part of the Hamiltonian,  $H_0$  is the diagonal part, here the "Ising energy"  $J \sum_{\langle ij \rangle} (S_i^z S_j^z - n_i n_j / 4)$ , and  $\Psi_0^g(\mathcal{S})$  is an approximate ground-state wavefunction which is used by the algorithm for importance sampling; the definition of  $r_{\mathcal{S}\mathcal{S}'}$ , Eq. (8), implies that the walks preferentially explore regions where  $|\Psi_0^g|$  is large. One calculates a weight factor associated with each walk, which is

$$w(\tau_1) = \exp(i\phi) \cdot \exp \left\{ - \int_0^{\tau_1} \left( H_0(\mathcal{S}(\tau)) - \sum_{\mathcal{S}'} r_{\mathcal{S}\mathcal{S}'} \right) d\tau \right\}. \quad (9)$$

This weight factor is a function of the path  $\mathcal{S}(\tau)$  followed by the walk, and in general has an overall phase  $\exp(i\phi)$ . When averaged over random walks the weight asymptotically approaches an exponential in the ground state energy,

$$\lim_{\tau \rightarrow \infty} \langle w(\tau) \rangle = c \exp(-E_0 \tau). \quad (10)$$

One may therefore determine energies from the average weight at two Euclidean times,

$$E_0^{estm} = \lim_{\tau_1, \tau_2 \rightarrow \infty} \ln \left( \langle w(\tau_1) \rangle / \langle w(\tau_2) \rangle \right) / (\tau_2 - \tau_1). \quad (11)$$

In practice there are biases due to the use of a finite sample of walks, a finite Euclidean step size  $h_\tau$  and finite measurement times  $\tau_1$  and  $\tau_2$ , and one must be careful to establish that these systematic errors are within required limits.

The weight phase  $\exp(i\phi)$  is the phase of the product of  $(-H_I)$  matrix elements encountered in all transitions executed by the walk;

$$\exp(i\phi) = \prod_{\substack{\mathcal{S} \rightarrow \mathcal{S}' \\ \text{transitions}}} \frac{-\langle \mathcal{S}' | H_I | \mathcal{S} \rangle}{|\langle \mathcal{S}' | H_I | \mathcal{S} \rangle|}. \quad (12)$$

In problems such as the determination of the ground state energy of the Heisenberg antiferromagnet we minimise statistical errors by choosing our basis  $\{|\mathcal{S}\rangle\}$  so this phase is always +1, which requires that all nonzero off-diagonal Hamiltonian matrix elements be negative. In the t-J model with a  $\hat{z}$ -diagonal spin basis this is not possible in general, and in any case we must introduce complex basis phases to extract dispersion relations.

To motivate our choice of basis phases, first consider a zeroth-order set of one-hole basis states  $\{|\mathcal{S}\rangle_0\}$  defined by applying a site-ordered string of fermion operators  $c_{n,s_z}^\dagger$  to the vacuum. For example, our initial Néel-and-hole state on the  $4 \times 4$  lattice, with the hole at site 1,  $\vec{x}_h = (0, 0)$ , is

$$|\mathcal{N}(0, 0)\rangle_0 = c_{2-}^\dagger c_{3+}^\dagger c_{4-}^\dagger c_{5-}^\dagger \dots c_{16+}^\dagger |0\rangle. \quad (13)$$

(Our sites are labelled as in Figure 1 of Dagotto *et al*<sup>18</sup>.) The phases of this basis are inappropriate for Monte Carlo simulations of the Heisenberg antiferromagnet, since every spin flip has a positive  $H_I$  matrix element and hence induces a change in sign of the weight factor. The solution of this problem is well known, and is to introduce a new basis set  $\{|\mathcal{S}\rangle_1\}$  with overall phases of  $(-1)^{N_{sf}}$ , where  $N_{sf}$  is the number of spin-flips required to reach the basis state starting from a reference Néel state. In our one-hole problem this specifies the *relative* phases *within each subset* of one-hole basis states  $\{|\mathcal{S}, \vec{x}_h\rangle_1\}$  that share the same hole location  $\vec{x}_h$ . Note however that we are still free to specify the overall phase of each of these basis subsets. It is this freedom that allows us to extract the dispersion relation for the hole, since this relative phase is determined by the total momentum of the state.

Momentum eigenstates are defined by their behavior under translations; a translation of a state of momentum  $\vec{k}$  by  $\vec{a}$  returns the same state with a  $\vec{k}$ -dependent phase,

$$T(\vec{a}) |\vec{k}\rangle = e^{-i\vec{k}\cdot\vec{a}} |\vec{k}\rangle. \quad (14)$$

We use this property of momentum eigenstates to choose our basis phases so that all states with momenta other than a specified  $\vec{k}$  are projected out in the sum over final hole sites, this sum being implicit in the calculation of the average weight  $\langle w \rangle$  in Eq. (10). Specifically, we use as our basis states translations of states with the hole at the origin, with a multiplicative phase factor of  $\exp\{+i\vec{k}\cdot\vec{a}\}$ . For example, to extract  $\vec{k} = (0, 0)$  energies, the basis state corresponding to a Néel-and-hole state with the hole at  $\vec{x}_h = (1, 0)$  is taken to be the pure translated state  $T|\mathcal{N}\rangle_0$ ,

$$\begin{aligned} T(\vec{x}_h = \hat{x}) |\mathcal{N}(0, 0)\rangle_0 &= c_{3-}^\dagger c_{4+}^\dagger c_{1-}^\dagger c_{6-}^\dagger \dots c_{13+}^\dagger |0\rangle \\ &= (-1) \cdot c_{1-}^\dagger c_{3-}^\dagger c_{4+}^\dagger c_{5+}^\dagger \dots c_{16-}^\dagger |0\rangle = (-1) \cdot |\mathcal{N}(1, 0)\rangle_0. \end{aligned} \quad (15)$$

Similarly, the  $\vec{k} = (0, 0)$  Néel-and-hole basis state with hole location  $(n_x, n_y)$  is

$$T(n_x \hat{x} + n_y \hat{y}) |\mathcal{N}(0, 0)\rangle_0 = (-1)^{n_x} |\mathcal{N}(n_x, n_y)\rangle_0. \quad (16)$$

(The factor of  $(-1)^{n_x}$  in Eqs. (15) and (16) is induced by the ordering convention, Eq. (13), used to define the  $\{|\mathcal{N}\rangle_0\}$  basis.) In contrast, to extract general  $\vec{k}$  states we use basis states with plane-wave phases, so that all states with  $\vec{K} \neq \vec{k}$  are eliminated in the average over final hole locations because  $\sum_{\vec{x}_h} \exp\{i(\vec{k} - \vec{K}) \cdot \vec{x}_h\}$  vanishes unless  $\vec{K} = \vec{k}$ . The required Néel-and-hole basis states with general  $\vec{k}$  and hole location  $(n_x, n_y)$  are

$$\begin{aligned} \exp(+i\vec{k} \cdot \vec{x}) T(n_x \hat{x} + n_y \hat{y}) |\mathcal{N}(0, 0)\rangle_0 \\ = \exp(+i(k_x n_x + k_y n_y)) (-1)^{n_x} |\mathcal{N}(n_x, n_y)\rangle_0. \end{aligned} \quad (17)$$

Previously we specified the relative phases within each fixed-hole-location subbasis  $\{|\mathcal{S}, \vec{x}_h\rangle\}$  by the Heisenberg-model  $(-1)^{N_{sf}}$  rule. As we have now specified the relative phases of specific basis states from each of these subbases by Eq. (17), the relative phases of all basis states are now determined.

The weight-factor phase, Eq. (12), equals the phase of the product of  $-H_{hop}$  matrix elements, Eq. (1), between the basis states, Eq. (17), where the product runs over all hole hops which the random walk has allowed. (We have chosen our phases so spin flips do not change the phase, Eq. (12); only hole hops remain as nontrivial  $-H_I$  terms in Eq. (12).) Inspection of Eqs. (13) and (17) shows that fermion operator ordering introduces an additional factor of  $(-1)$  in the matrix element of  $(-H_I)$  for each hole hop in the  $\pm\hat{y}$  directions. This factor combined with the phase multiplying Eq. (17) gives the total weight-factor phase  $\exp(i\phi)$  we use in Eqs. (9) and (11) to determine the hole dispersion relation.

As this definition of phases is somewhat complicated, it may be useful to specify the resulting rule for the weight-factor phase  $\exp(i\phi)$  in Eq. (9) operationally:

(i) spin flips have no effect on the phase, (ii) under a hole hop the phase of the weight changes by a factor of

$$e^{i\Delta\phi} = (-1) \cdot e^{-i\vec{k} \cdot \Delta\vec{x}_h} \cdot (-1)^{\Delta N_{sf}} . \quad (18)$$

The overall  $(-1)$  is the product of the intrinsic  $(-1)$  in Eq. (16) encountered in translating the “zerth order” basis states as in Eq. (13) by  $\pm\hat{x}$  times the operator-ordering phase  $(-1)$  encountered for hole hops along  $\pm\hat{y}$ ; their combined effect is a  $(-1)$  for every hole hop. The second factor is due to the  $\exp(i\vec{k} \cdot \vec{x}_h)$  present in a momentum eigenstate. The third factor is the Heisenberg minus sign which insures that spin flips never change the sign of the weight. All these may simply be evaluated as an overall phase factor of

$$e^{i\phi(\vec{k})} = (-1)^{N_{hops}} \cdot e^{-i\vec{k} \cdot (\vec{x}_h(f) - \vec{x}_h(i))} \cdot (-1)^{\Delta N_{sf}} , \quad (19)$$

at the end of each walk (at  $\tau_1$  or  $\tau_2$ ); note that the first two phase factors on the rhs depend only on the initial and final configurations, not on the path followed. The average weight and resulting energy for each momentum can then be calculated using Eqs. (9), (11) and (19) for each  $\vec{k}$ . Note that the energies for all momenta are determined concurrently by evaluating average weights with different end-point factors of  $\exp(i\phi(\vec{k}))$ .

### 3. Perturbation Theory

At the present time, the large hopping parameters of high temperature superconductivity are inaccessible to the GRW because of the minus sign problem. One way to study this regime is to fit the small  $t/J$  regime where simulations can be done with a perturbative form which may then be used to extrapolate to larger values of the hopping parameter.

Although no numerical results have previously appeared for the t-J model bandwidth on lattices larger than 20 sites, there are theoretical arguments that the one-hole band structure at small  $t/J$  should depend strongly on the lattice size<sup>19-21</sup>. Perturbation theory in the hopping parameter<sup>18,20,21</sup> finds that the small- $t/J$  dispersion relation is

$$e_h(\vec{k}, t) = e_h(t=0) + Z_w \cdot 2t [\cos(k_x) + \cos(k_y)] + O(t^2/J) , \quad (20)$$

where  $Z_w$  is a bandwidth renormalization; the small- $t/J$  bandwidth is  $W = Z_w \cdot 8t$ .  $Z_w = +1$  for a free fermion on the lattice, and for the hole it is a function of both  $S_{tot}$  and  $L$ , and involves an overlap of initial and final spin-wavefunctions<sup>21</sup>. It has been suggested that this bandwidth renormalization is actually zero in the bulk limit<sup>19</sup>, although probably only for low-spin states<sup>21</sup> ( $S_{tot}/L^2 \rightarrow 0$ ), because the staggered-magnetized spin background reduces the overlap between one-hop initial and final spin states to zero. This effect has also been attributed to a dimerization of the lattice by the staggered magnetization in the bulk limit<sup>19</sup>, which reduces the size of

the effective Brillouin zone and leads to degeneracies between levels with momenta that differ by  $(\pi, \pi)$ . This implies  $Z_w = 0$ , so the bulk-limit bandwidth at leading order in the hopping parameter expansion is  $O(t^2/J)$ . At large but finite  $L$ , simple arguments involving the spin-wave gap (which vanishes  $\propto 1/L^2$ ) and degeneracies expected at the supersymmetric point <sup>21-23</sup> ( $t/J = 1/2$ ) lead one to expect that  $Z_w$  for the low-spin states should approach zero as  $\kappa/L^2$ .

One-hole band structure at second order in the hopping parameter has been discussed by Dagotto, Joynt, Moreo, Bacci and Gagliano <sup>18</sup>, who obtained a general three-parameter form for the  $O(t^2/J)$  one-hole dispersion relation. Their equation (20) is equivalent to the form

$$e_h(\vec{k}, t)/J = v_1 + v_2 [\cos(k_x) + \cos(k_y)] \cdot \left(\frac{t}{J}\right) + \left\{ v_3 [\cos^2(k_x) + \cos^2(k_y)] + v_4 [\cos(k_x) \cos(k_y)] + v_5 \right\} \cdot \left(\frac{t}{J}\right)^2. \quad (21)$$

There is a relation between the coefficients  $\{v_i\}$  in  $O(t^2/J)$  perturbation theory, which is implicit in their definition in terms of the  $\{\alpha_i\}$  of Dagotto *et al*,

$$v_2 = 2Z_w = -2\alpha_0, \quad (22)$$

$$v_3 = -\frac{8(\alpha_1^2 + \alpha_2)}{\alpha}, \quad (23)$$

$$v_4 = -\frac{16\alpha_1(1 + \alpha_2)}{\alpha}, \quad (24)$$

$$v_5 = -\frac{4(1 - \alpha_2)^2}{\alpha}, \quad (25)$$

where

$$\alpha \equiv \frac{3}{2} - \frac{9}{2}\alpha_0 + 2\alpha_1 + \alpha_2. \quad (26)$$

In our fits to numerical results we do not impose the constraint but instead treat all five coefficients  $\{v_i\}$  as free parameters.

#### 4. Implementation on the iPSC/860 hypercube

To implement the GRW on the Intel IPSC/860 we subdivided the total number of random walks in each sample into blocks of 4 million walks which were then divided among 32 nodes. The host program performed the I/O, reading the input parameters and the output, and handled the communication with the nodes. The random number generator was initialized with a different seed on each node on which independent sets of random walks were then generated. At the end, the results from the independent runs were sent back to the host where they were averaged to give energy estimates for the 4 million walk blocks which were themselves averaged to give estimates for

all walks in the sample. No communication between nodes was required because the GRW algorithm requires only a single configuration, so the memory requirements were very small and each node was used as an independent processor during the simulation. Each of these 4 million walk blocks took approximately 3 and 6 hours per node on the 4x4 and 6x6 lattices respectively at  $\tau = 6.0$

## 5. Results and Discussion

In our simulations we studied the spectrum of single-hole states on  $4 \times 4$  and  $6 \times 6$  lattices. Lanczos results are known for the  $4 \times 4$  lattice, which served as a test case. For our initial configuration we used a Néel state with a hole at the origin. First, to confirm that the algorithm gives correct results we generated  $4 \times 4$  energies for the six independent momenta at small  $t/J$  values of 0.0, 0.025, 0.05, 0.075 and 0.10. For importance sampling we used a simple trial wavefunction of the form

$$|\psi_0^g(\mathcal{S})\rangle = c e^{-\xi H_0(\mathcal{S})}, \quad (27)$$

and an optimum parameter value of  $\xi \approx 0.56$  was found by minimizing the variance of weight-factor moduli. (This is slightly larger than the value used in previous static-hole simulations<sup>12</sup>.) After some numerical tests we chose to set  $\tau_1 = 6.0$ ,  $\tau_2 = 7.0$  and  $h_\tau = 0.025/L^2$  (the Euclidean times and  $h_\tau$  are given in units of  $J^{-1}$ ), and we generated samples of  $2^{22}$  random walks for each value of  $t/J$ . The average weights  $\langle w(\tau_1) \rangle$  and  $\langle w(\tau_2) \rangle$  are in general complex numbers, but as only the overall time dependence is relevant to the energy we used the modulus of the average weight  $|\langle w(\tau) \rangle|$  in Eq. (9). The resulting one-hole band is shown together with Lanczos results in Table 1 and Figure 1; evidently the results are numerically consistent.

We have added  $(\pi, \pi)$  to all the momenta before displaying the energies in the figure and table, to change the definition of momentum to that of references 5 and 20, and will use their convention in our subsequent discussion. The weight phases described in the text correspond to the momentum conventions of references 24 and 25. Our results are also consistent with the known degeneracy of the  $(\pi/2, \pi/2)$  and  $(\pi, 0)$  multiplets, which is due to a higher symmetry of the  $4 \times 4$  lattice and is not trivially realized in the Monte Carlo simulation.

Inspection of the weight-factor variance shows that the energy errors increase by about a factor of three with each step of  $\Delta(t/J) = 0.05$ , given these parameters and the simple trial wavefunction, Eq. (27). Since the errors decrease as  $1/\sqrt{N_{rw}}$ , to maintain the small statistical errors in Table 1 we must increase the sample of walks by about a factor of  $2^3$  for each step of  $\Delta(t/J) = 0.05$ . This is illustrated by the  $t/J = 0.15$  points, which are averages of  $2^{25}$  walks and in consequence have errors comparable to the  $t/J = 0.10$  points with  $N_{rw} = 2^{22}$ . For the final measurements at  $t/J = 0.20$  we again generated  $2^{25}$  walks, and the anticipated increase in error by approximately a factor of three relative to  $t/J = 0.15$  is evident. For most levels the error is still relatively small,  $\pm 0.005$  to  $\pm 0.012$ , but for the worst case of  $\vec{k} = (0, 0)$  we find a large error of about  $\pm 0.05$ . We emphasize that the rapid growth of statistical

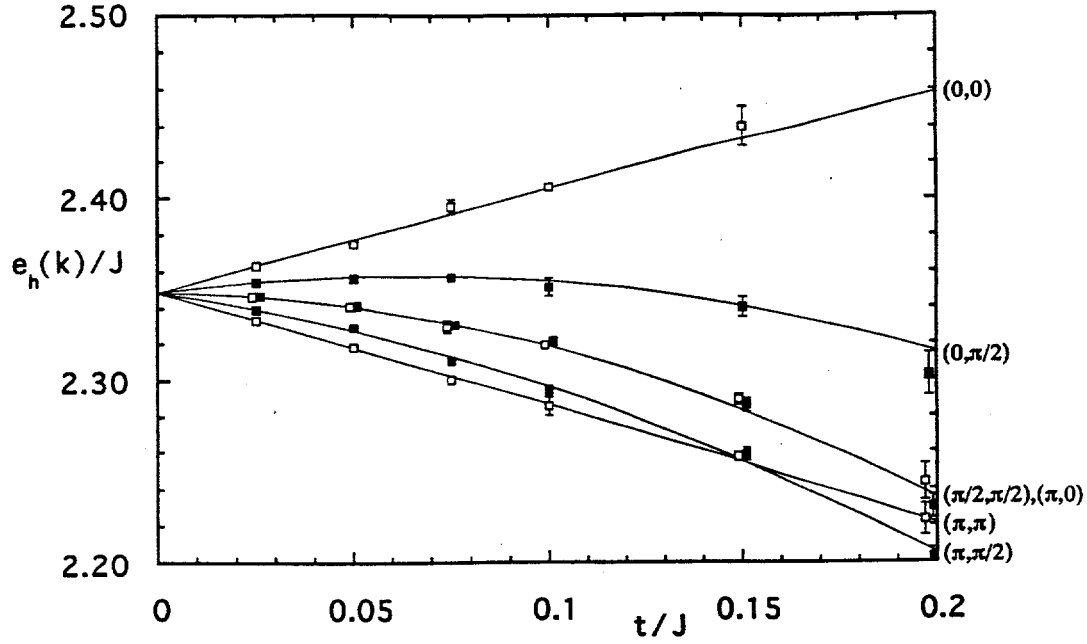


Figure 1. Lanczos and Monte Carlo results for the  $S_{\text{tot}}=1/2$  one-hole band on the  $4 \times 4$  lattice.

errors with  $t/J$  is due to the large Euclidean measurement time  $\tau_1$  used in these simulations. This large  $\tau_1$  is required to remove excited-state contributions from the very simple trial wavefunction, Eq. (27) used in this initial study. Improved Heisenberg-model wavefunctions with long-range correlations have been described in the literature (see for example section III.E. of the review by Manousakis<sup>17</sup> and papers by Liang, Doucot and Anderson<sup>26</sup> and Dagotto and Schrieffer<sup>27</sup>), and by incorporating such an improved wavefunction we anticipate that a much shorter evolution in Euclidean time will give comparably accurate results. As these will experience fewer hole hops, and hence smaller rotations of the weight phase, the “minus sign problem” will be considerably reduced.

On the  $4 \times 4$  lattice, the values of the coefficients  $\{v_i\}$  are found from Lanczos data, and in particular,

$$v_2 = 0.2976, \quad (28)$$

which indicates the linear- $t$  bandwidth narrowing relative to the free-fermion value,

$$Z_w(4 \times 4) = v_2/2 = 0.1488. \quad (29)$$

In figure 2a, we plot the one-hole band up to  $t/J = 0.5$  using the above fitted

Table 1: Lanczos and Monte Carlo results for the lowest-lying  $S_{tot} = 1/2$  one-hole band on the  $4 \times 4$  lattice; we display  $e_h(\vec{k})/J = (E_h(\vec{k}) - E_0)/J$  at each independent momentum versus  $t/J$ .

$t/J =$	0.025	0.050	0.075	0.100	0.150	0.200
$\vec{k} = (0, 0)$	2.36331 2.3631(8)	2.37779 2.3754(19)	2.39200 2.3958(40)	2.40593 2.4064(11)	2.43291 2.4397(109)	2.45864 2.5291(531)
$(\pi/2, 0)$	2.35456 2.3543(6)	2.35765 2.3566(18)	2.35780 2.3573(18)	2.35502 2.3517(49)	2.34077 2.3402(54)	2.31538 2.3030(118)
$(\pi, 0)$	2.34670 2.3463(6)	2.34112 2.3412(15)	2.33189 2.3300(34)	2.31911 2.3195(21)	2.28341 2.2895(31)	2.23529 2.2436(100)
$(\pi/2, \pi/2)$	2.34670 2.3468(6)	2.34112 2.3418(6)	2.33189 2.3309(14)	2.31911 2.3214(22)	2.28341 2.2863(36)	2.23529 2.2302(62)
$(\pi, \pi/2)$	2.33970 2.3393(4)	2.32804 2.3296(12)	2.31367 2.3111(15)	2.29670 2.2946(29)	2.25540 2.2590(32)	2.20513 2.2030(49)
$(\pi, \pi)$	2.33355 2.3331(7)	2.31829 2.3187(12)	2.30277 2.3007(21)	2.28700 2.2859(50)	2.25472 2.2576(23)	2.22145 2.2232(85)

coefficients, and compare to previous Lanczos results in Figure 2b. The qualitative agreement between the two plots is evident.

To study one-hole band structure on the  $6 \times 6$  lattice, for which no numerical results previously had been reported, we generated Monte Carlo energies for the 10 independent momentum levels using the same parameters and trial wavefunction as in the  $4 \times 4$  simulation. We measured energies at  $t/J = 0.0, 0.025, 0.050, 0.075$  and  $0.10$ , with  $2^{25}$  walks at each  $t/J$  value. The  $6 \times 6$  Heisenberg model ground-state energy with the same Monte Carlo parameters was found to be  $E_0 = -24.4406 \pm 0.0010$ , which is consistent with our previous Monte Carlo result<sup>12</sup> and with the recent Lanczos result of Schulz and Ziman<sup>28</sup>,  $E_0 = -24.4394$ . In the  $6 \times 6$  one-hole systems however we found somewhat slower convergence of Monte Carlo energies with Euclidean time, and in the static-hole case we estimate the resulting bias due to running at  $\tau_1 = 6$  to be  $\Delta E \approx +0.023$ . We have added this systematic correction to our measured energies, and the resulting final estimates are shown *with statistical errors only* in Figure 3. The complete details of our  $6 \times 6$  results are presented in ref. 6.

The uncertainty in this bias is about  $\pm 0.005$ , which is somewhat larger than the statistical errors of most of the  $6 \times 6$  one-hole energies. Thus, our errors are dominantly systematic rather than statistical.

To provide a parametrization of the  $6 \times 6$  band and to extrapolate to larger  $t/J$

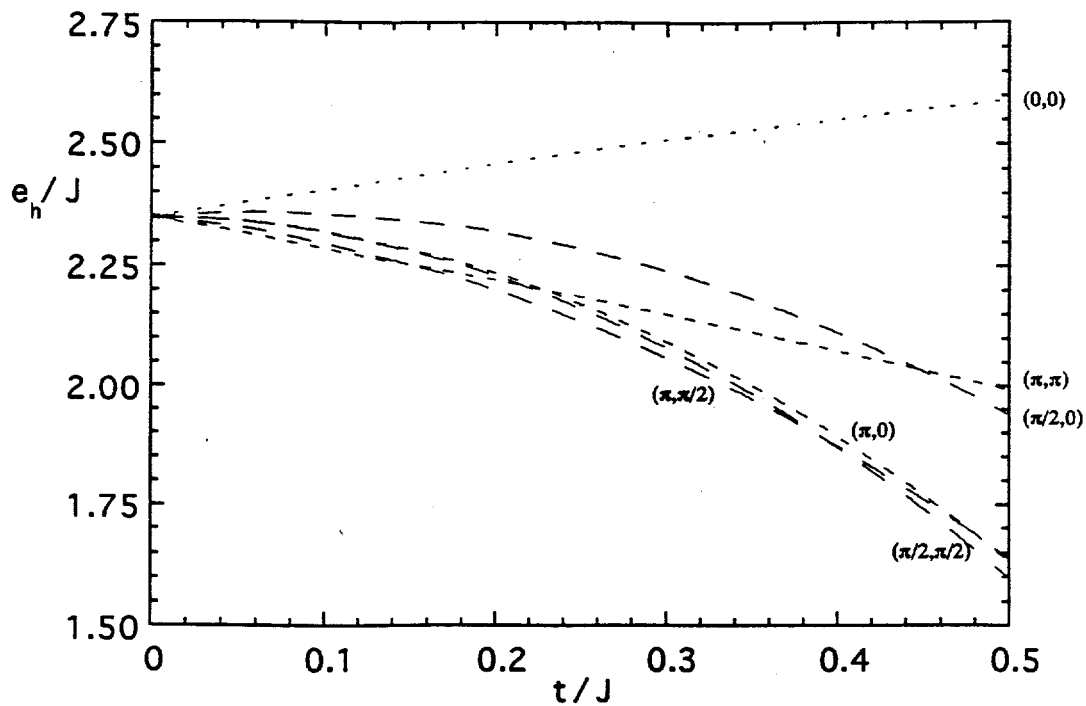


Figure 2a. Extrapolation of the one-hole band to  $t/J=0.5$  using the fitted coefficients.

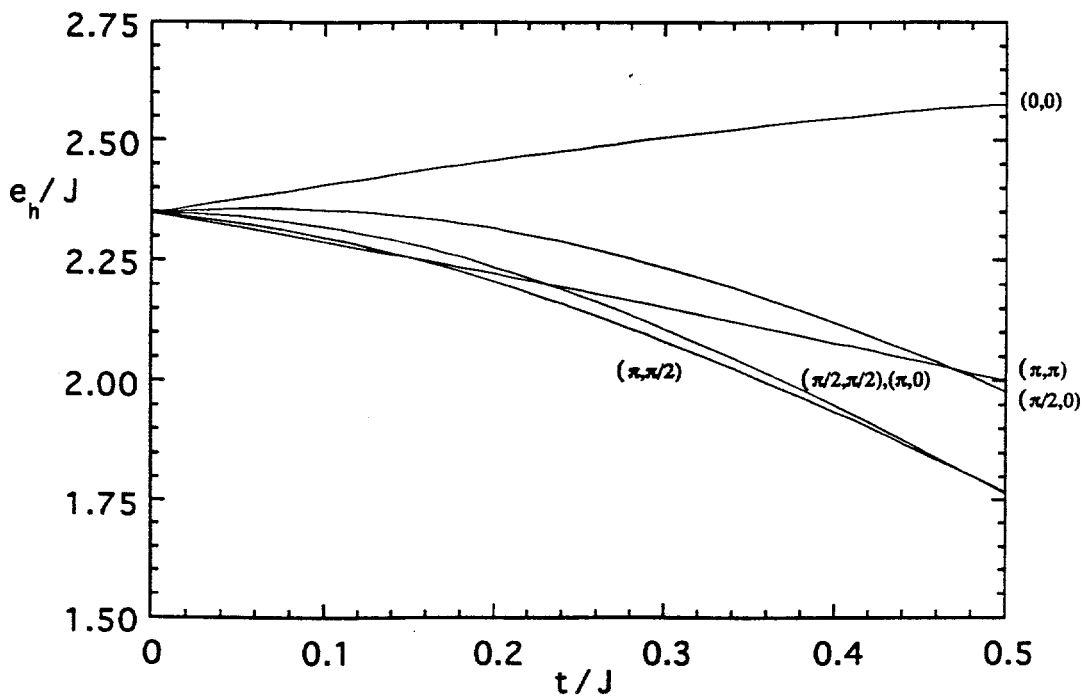


Figure 2b. Lanczos results for the  $S_{\text{tot}}=1/2$  one-hole band

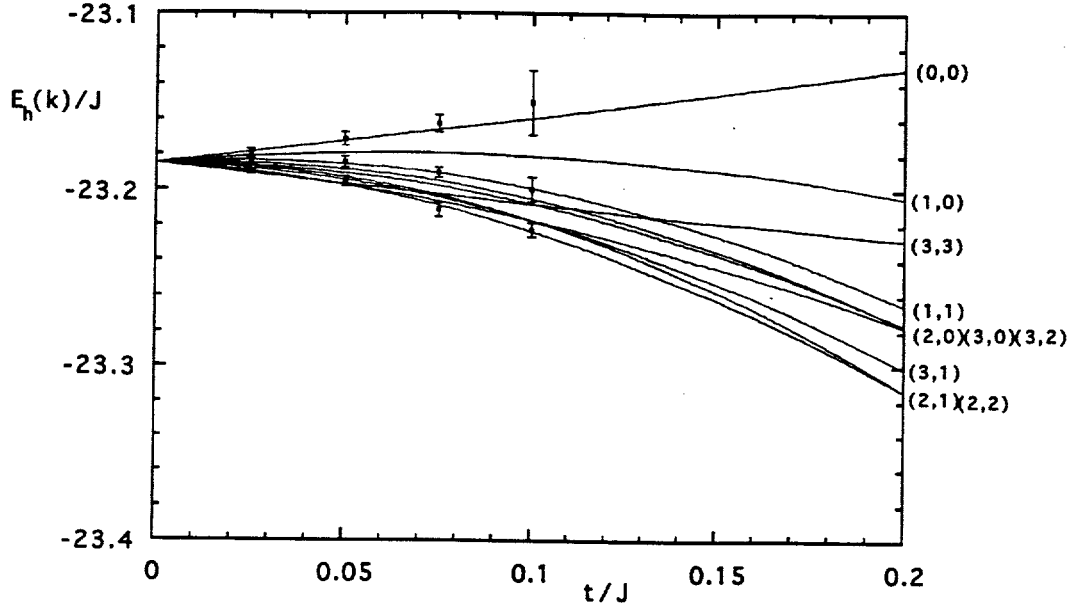


Figure 3. Monte Carlo results for three  $6 \times 6$  levels and fitted curves for all levels.  $(n_x, n_y)$  denotes momentum  $(n_x \pi/3, n_y \pi/3)$ ; only  $(0,0)$ ,  $(1,1)$  and  $(2,2)$  data points are displayed.

we carried out a least-squares fit of the  $6 \times 6$  data to the  $O(t^2/J)$  hopping parameter expansion, Eq. (21). The  $4 \times 4$  (Figure 1) and  $6 \times 6$  (Figure 3) bands are plotted on the same scale; comparison of these figures clearly shows evidence for band narrowing on the larger lattice. To avoid confusion in Figure 3 we show Monte Carlo results only for three representative levels, which in order of increasing energy are  $(2\pi/3, 2\pi/3)$ ,  $(\pi/3, \pi/3)$  and  $(0, 0)$ ; the latter generally has the largest statistical errors. We also show the fitted band energies, Eq. (21), for all levels.

From our numerical fits to the perturbative form, Eq. (21), bandwidth renormalization indicates band narrowing:

$$Z_w = \begin{cases} 1, & \text{free fermion whooshing around} \\ 0.150(5), & 4 \times 4 \\ 0.061(5), & 6 \times 6 \\ 0.065, & 6 \times 6 \text{ from supersym. arguments} \\ 0, & \text{static hole} \end{cases} \quad (30)$$

This numerical result clearly supports the conjecture that the linear- $t$  component of the one-hole bandwidth vanishes in the bulk limit.

We find that the hopping-parameter expansion, Eq. (21), with numerically determined coefficients gives a qualitatively correct picture of the  $4 \times 4$  band to  $t/J \sim 0.5$ . It may therefore be of interest to present our extrapolated results for the  $6 \times 6$  band for comparison with future Monte Carlo studies. Our result obtained with the fitted coefficients is shown in Figure 4 for the range  $0 \leq t/J \leq 0.5$ . Note that the  $(2\pi/3, \pi/3)$  level is expected to be the  $6 \times 6$  ground state at moderate  $t/J$  because it is closest in energy to the  $(\pi/2, \pi/2)$  minimum of the  $O(t^2/J)$  terms in Eq. (21).

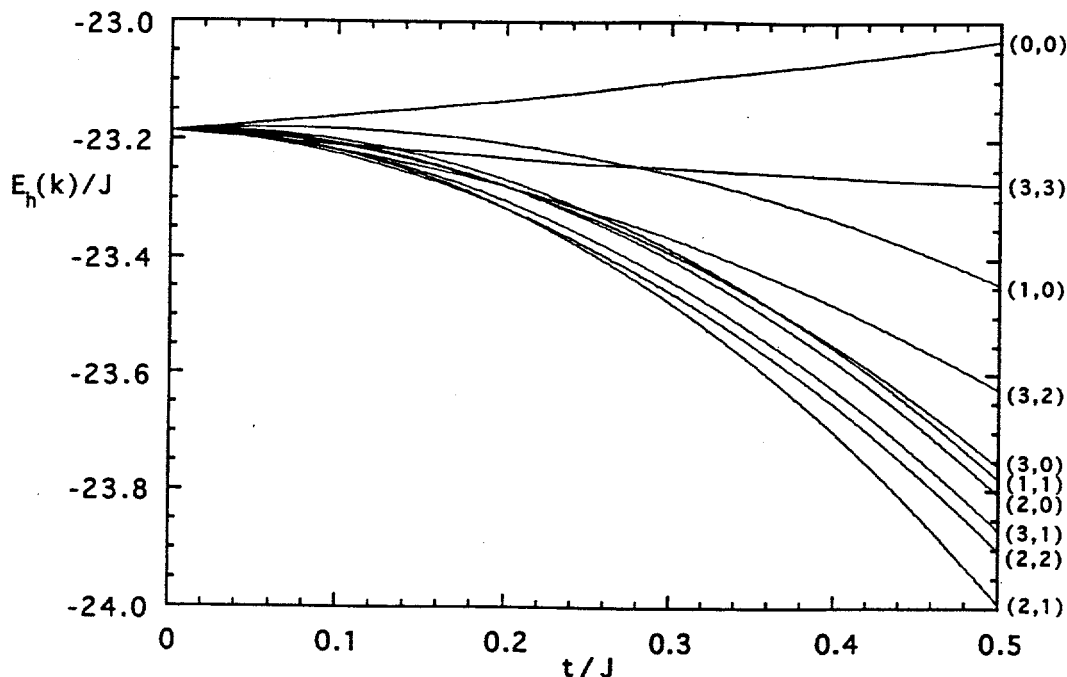


Figure 4. 6x6 t-J band structure from extrapolated Monte Carlo data.  $(n_x, n_y)$  denotes momentum  $(n_x \pi/3, n_y \pi/3)$ .

As a result of the simple importance sampling, Eq. (27), used here, we cannot at present resolve band structure at appreciably larger values of  $t/J$ , but we anticipate that this will be possible given an improved trial wavefunction. This has been demonstrated by Boninsegni and Manousakis<sup>2</sup>, who used a trial wavefunction with long-range correlations in a similar Monte Carlo algorithm and were able to follow the  $(\pi/2, \pi/2)$  one-hole level to  $t/J = 5$  on large lattices. The advantage of using a more accurate spin wavefunction is that convergence to the ground state to a specified accuracy occurs at a smaller Euclidean time, in which fewer hole hops take place. In consequence one may carry out Monte Carlo measurements at appreciably larger values of  $t/J$ . In future we plan to extend our Monte Carlo study of band structure in the t-J model to values relevant to the superconductors through the incorporation of similar improved importance sampling.

## 6. Acknowledgements

We would like to thank E.Dagotto, V.Elser, D.Huse, A.E.Jacobs, R.Joynt, S.Liang, E.Manousakis, A.Moreo, E.S.Swanson and T.A.L.Ziman for useful discussions of various aspects of this work. This research was sponsored by the United States Department of Energy under contract DE-AC05-84OR21400 and through the Quantum Structure of Matter project also funded by the Department of Energy at Oak Ridge National Laboratory, by project 3210-0427 with Martin Marietta Energy Systems Inc, and by the State of Tennessee Science Alliance Center under contract R01-1062-32.

## 7. References

1. E.Y.Loh, J.E.Gubernatis, R.T.Scalettar, S.R.White, D.J.Scalapino and R.L.Sugar, *Phys. Rev.* **B41**, 9301 (1990).
2. M.Boninsegni and E.Manousakis, Florida State University report FSU-SCRI-92-12 (January 1992).
3. M.Takahashi, *Phys. Rev. Lett.* **62**, 2313 (1989).
4. J.E.Hirsch, *Phys. Rev. Lett.* **54**, 1317 (1985); E.Dagotto, *Int. J. Mod. Phys.* **B5**, 907 (1991).
5. E.Dagotto, A.Moreo and T.Barnes, *Phys. Rev.* **B40**, 6721 (1989);
6. This paper is based on an article to appear in Physical Review B, Oak Ridge National Laboratory report ORNL-CCIP-92-03.
7. T.Barnes, G.J.Daniell and D.Storey, *Nucl. Phys.* **B265** [FS15] (1986) 253.
8. T.Barnes and G.J.Daniell, *Phys. Rev.* **B37**, 3637 (1988); see also T.Barnes, in Proceedings of *Computational Atomic and Nuclear Physics at One Gigaflop*, C.Bottcher, M.R.Strayer and J.McGrory eds., Vol.16, *Nuclear Science Research Conference Series* (Harwood Academic, 1989) pp.83-106.
9. T.Barnes and E.S.Swanson, *Phys. Rev.* **B37** (1988) 9405.
10. T.Barnes and D.Kotchan, *Phys. Rev.* **D35** (1987) 1947; D.Kotchan, University of Toronto Ph.D. thesis (1990).
11. G.Gronzin, "A Monte Carlo Study of the Light  $q^2\bar{q}^2$  System", in Proceedings of the IVth International Conference on Hadron Spectroscopy *HADRON '91*, pp.783-788; eds. S.Oneda and D.C.Peaslee (World Scientific, 1992); University of Toronto Ph.D. thesis, in preparation.
12. T.Barnes and M.D.Kovarik, *Phys. Rev.* **B42**, 6159 (1990).
13. T.Barnes, K.J.Cappon, E.Dagotto, D.Kotchan and E.S.Swanson, *Phys. Rev.* **B40**, 8945 (1989).
14. T.Barnes, E.Dagotto, J.Riera and E.S.Swanson, *Phys. Rev.* **B47**, 3196 (1993).
15. T.Barnes, E.Dagotto, A.Moreo and E.S.Swanson, *Phys. Rev.* **B40**, 10997 (1989).
16. T.Barnes, *Int. J. Mod. Phys.* **C2**, 659 (1991).
17. E.Manousakis, *Rev. Mod. Phys.* **63**, 1 (1991).
18. E.Dagotto, R.Joynt, A.Moreo, S.Bacci and E.Gagliano, *Phys. Rev.* **B41**, 9049 (1990).
19. V.Elser, D.A.Huse, B.I.Shraiman and E.D.Siggia, *Phys. Rev.* **B41**, 6715 (1990).
20. T.Barnes, A.E.Jacobs, M.D.Kovarik and W.G.Macready, *Phys. Rev.* **B45**, 256 (1992).
21. T.Barnes, "The t-J Model at Small t/J: Numerical, Perturbative and Supersymmetric Results", Oak Ridge report ORNL-CCIP-91-03, in Proceedings of the University of Miami Workshop on Electronic Structure and Mechanisms for High Temperature Superconductivity *High-Temperature Superconductivity; Physical Properties, Microscopic Theory, and Mechanisms*, eds. J.Ashkenazi, S.E.Barnes, F.Zuo, G.C.Vezzoli and B.M.Klein (Plenum, 1992), pp. 503-513.
22. D.Förster, *Int. J. Mod. Phys.* **B3**, 1783 (1989).

23. K.J.Cappon, *Phys. Rev.* **B43**, 8698 (1991).
24. Y.Hasegawa and D.Poilblanc, *Phys. Rev.* **B40**, 9035 (1989).
25. J.Bonca, P.Prelovsek and I.Sega, *Phys. Rev.* **B39**, 70 (1989).
26. S.Liang, B.Doucot and P.W.Anderson, *Phys. Rev. Lett.* **61**, 365 (1988).
27. E.Dagotto and J.R.Schrieffer, *Phys. Rev.* **B43**, 8705 (1991).
28. H.J.Schulz and T.A.L.Ziman, *Euro. Phys. Lett.* **18**, 355 (1992).

#### DISCLAIMER

This report was prepared as an account of work sponsored by an agency of the United States Government. Neither the United States Government nor any agency thereof, nor any of their employees, makes any warranty, express or implied, or assumes any legal liability or responsibility for the accuracy, completeness, or usefulness of any information, apparatus, product, or process disclosed, or represents that its use would not infringe privately owned rights. Reference herein to any specific commercial product, process, or service by trade name, trademark, manufacturer, or otherwise does not necessarily constitute or imply its endorsement, recommendation, or favoring by the United States Government or any agency thereof. The views and opinions of authors expressed herein do not necessarily state or reflect those of the United States Government or any agency thereof.